# ESS nBLM: Beam Loss Monitors based on fast neutron detection

Thomas Papaevangelou, Helder Alves, Stephan Aune, Vincent Gressier, Joel Beltramelli, Quentin Bertrand, Thomas Bey, Benoit Bolzon, Nicolas Chauvin, Michel Combet, et al.

ISBN: 978-3-95450-202-8 doi:10.18429/JACoW-HB2018-THA1WE04



# ESS nBLM: BEAM LOSS MONITORS BASED ON FAST NEUTRON DETECTION

T. Papaevangelou†, H. Alves. S. Aune, J. Beltrameli, Q. Bertrand, B. Bolzon, M. Combet, T. Bey, N. Chauvin, D. Desforge, M. Desmons, Y. Gauthier, E. Giner-Demange, A. Gomes, F. Gougnaud, F. Harrault, F. J. Iguaz, T. Joannem, M. Kebbiri, C. Lahonde-Hamdoun, P. Le Bourlout, P. Legou, O. Maillard, Y. Mariette, A. Marcel, J. Marroncle, C. Marchand, M. Oublaid ,V. Nadot, G. Perreu, O. Piquet, B. Pottin, Y. Sauce, L. Segui, F. Senée, J. Schwindling, G. Tsiledakis, R. Touzery, O. Tuske, D. Uriot, IRFU, CEA, Université Paris-Saclay, F-91191 Gif-sur-Yvette, France
M. Pomorski, CEA-LIST, Diamond Sensors Laboratory, F-91191, Gif sur Yvette, France
I. Dolenc-Kittelmann, R. Hall-Wilton[1], C. Höglund[2], L. Robinson, P. Svensson, T. J. Shea, European Spallation Source ERIC, SE-221 00, Lund, Sweden
[1]also Mid-Sweden University, SE-851 70, Sundsvall, Sweden
[2]also Thin Film Physics Division, Department of Physics, Chemistry and Biology (IFM), Linköping University, SE-581 83 Linköping, Sweden
V. Gressier., IRSN, BP3, 13115 Saint-Paul-Lez-Durance, France
K. Nikolopoulos, School of Physics and Astronomy, University of Birmingham, B15 2TT, UK

*Abstract*

A new type of Beam Loss Monitor (BLM) system is being developed for use in the European Spallation Source (ESS) linac, primarily aiming to cover the low energy part (proton energies between 3-100 MeV). In this region of the linac, typical BLM detectors based on charged particle detection (i.e. Ionization Chambers) are not appropriate because the expected particle fields will be dominated by neutrons and photons. Another issue is the photon background due to the RF cavities, which is mainly due to field emission from the electrons from the cavity walls, resulting in bremsstrahlung photons. The idea for the ESS neutron sensitive BLM system (ESS nBLM) is to use Micromegas detectors specially designed to be sensitive to fast neutrons and insensitive to low energy photons (X and gammas). In addition, the detectors must be insensitive to thermal neutrons, because those neutrons may not be directly correlated to beam losses. The appropriate configuration of the Micromegas operating conditions will allow excellent timing, intrinsic photon background suppression and individual neutron counting, extending thus the dynamic range to very low particle fluxes.

## INTRODUCTION

The high intensity of the ESS beam implies that even a loss of a small fraction of the beam could result in significant irradiation and destruction of accelerator equipment. The Beam Loss Monitor systems must be capable of detecting the smallest possible fraction of beam loss, approaching 0.01 W/m loss, preventing activation of machine components and allowing hands-on maintenance. Two types of BLM systems will be deployed, each providing unique capabilities [1-3]. The first type is based on an ionization chamber (ICBLM) [4], a simple and proven detector, but with reduced ability to discriminate beam losses in the low energy part of the linac against background from the accelerating structures [5]. The second type (nBLM) is based on a neutron sensitive detector with a Micromegas readout [6]. This is a system of higher complexity, but with the ability to discriminate between neutrons produced by loss of low energy protons, and photons produced by field emission in the cavities.

The two systems will cover the linac complementarily, with the nBLM aiming primarily to cover the low energy part of the accelerator (up to 90MeV) and the ICBLM the high energy part. Monte Carlo simulations are used to optimize the locations of the detectors, such that coverage and redundancy are provided for machine protection and spatial resolution is provided for diagnostic purposes [7].

## THE ESS NBLM SYSTEM

Micromegas [8, 9] is a Parallel Plate Detector (PPD) with three electrodes, cathode, micromesh and anode. The micromesh separates the two regions of the detector: the conversion or drift region between the cathode and the micromesh where the primary ionization occurs and the amplification region between the micromesh and the anode, which is narrow, typically 50-100 microns wide. Since its invention in 1996 by I. Giomataris and G. Charpak, Micromegas has been used in many different applications and particle physics experiments. As all Micro Pattern Gaseous Detectors (MPGD), Micromegas offers robustness, high gain, fast signals, high rate capabilities, better aging properties, low cost and simplified manufacturing processes compared to traditional gaseous detectors.

The flexibility in the choice of the gas, the operating conditions and the construction materials allows us to tune the sensitivity of the detector to the different particles and adapt its response to specific experimental requirements. Using appropriate neutron-to-charge converters and neutron absorbing materials, it is possible to adapt the detector to a wide range of neutron measurements [10].

† email address : thomas.papaevangelou@cea.fr

ISBN: 978-3-95450-202-8 doi:10.18429/JACoW-HB2018-THA1WE04

### *Micromegas for Neutron Detection*

The Micromegas detectors for the ESS nBLM system are specifically designed to be sensitive to fast neutrons and intrinsically insensitive to photons (X- and γ-rays), while signals from thermal neutrons are suppressed.

The detection of the fast neutrons is performed with two different approaches (Figure 1). In one approach we use a hydrogen rich convertor in order to detect the proton recoils that are created by the elastic scattering of the incoming neutrons. In this setup, the detector is intrinsically blind to low energy neutrons because only the fast ones ($E_n$ > ~0.5 MeV) can create recoils with significant range to enter the detector drift region. The suppression of gammas is based on the much smaller ionization of the gas by the photo-electrons compared to proton recoils. This kind of detector has a preferred direction for neutron detection, while the efficiency ranges between $10^{-5}$ – $10^{-3}$ for neutron energies 0.5 - 10 MeV. The timing response of such detector is very fast (at the level of ns) and the duration of a neutron induced signal is of the order of 50 - 100 ns.

In the second approach we use as convertor a material with high (n, α) cross-section, such as $^{10}$B and we surround the detector with a neutron moderator (i.e. polyethylene). In order to reject incoming slow neutrons, we use an external neutron absorber like boron-rich rubber, with the cut-off energy determined by the absorber thickness. The gamma rejection is based again on the difference in the ionization between electrons and alphas or heavier ions. Such a detector has 4π acceptance for neutrons. The detection efficiency is practically constant over a large energy range (from eV up to tens of MeV) and as high as few %. However, the neutron moderation process will delay a big part of the events for times from some 10 ns to 200 μs.

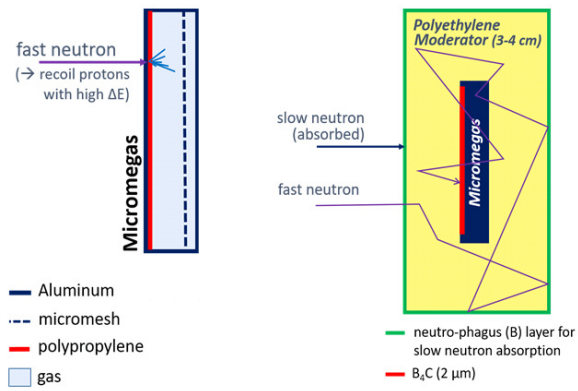


Figure 1: Neutron detection principle of the "fast" (left) and of the slow detector (right).

Both detectors will be operated in counting mode, being thus sensitive to individual neutrons, but in case of very high fluxes they will pass automatically to current mode.

### *Detector of the ESS nBLM System*

A common design has been adopted for both fast and slow detector chambers, the only difference being the cathode (drift) electrode. In the case of the fast detector it is a 125 μm Mylar foil with an aluminum deposit of 50 nm in order to apply the polarization voltage. This was preferred to aluminized polypropylene (1 mm thick) due to the long term stability of the aluminum layer, though it is less efficient for neutron detection by a factor ~2. The foil is glued to an aluminum plate for robustness.

In the case of the slow detector, the drift electrode consists of an Al plate that is coated with $^{10}B_4C$. Various thicknesses between 0.2 and 1.5 μm were chosen, allowing to tune the detector by up to a factor of 7.5. The samples were prepared using direct current magnetron sputtering from $^{10}B_4C$ sputtering targets (with a $^{10}$B enrichment of > 96%) in an industrial coating unit (CC800/9, CemeCon AG, Germany) in the ESS Detector Coatings Workshop in Linköping, Sweden. The coating parameters were similar to the ones used in [11-13] and fulfill the requirements for film purity, homogeneity, and long-term stability.

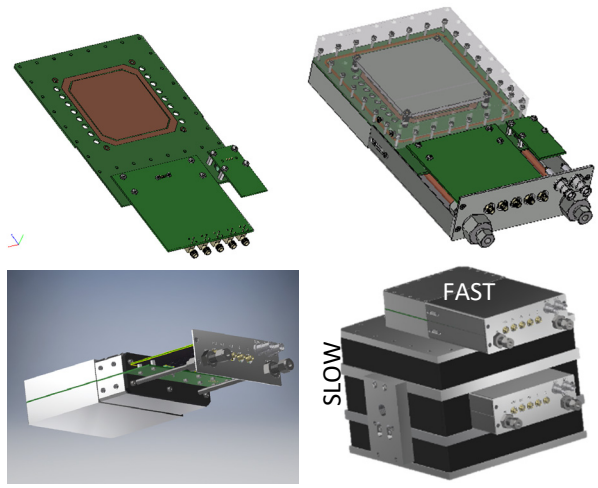


Figure 2: Schematic view of the Micromegas readout and chamber. Assembly of one fast and one slow detector including polyethylene moderator and borated rubber absorber.

The active area of the detector is 8 × 8 cm$^2$, segmented in 4 strips that can be read independently or as one. The Micromegas is built with the standard bulk technique [14] and is filled with a mixture of He + i$C_4H_{10}$ (10%). The aluminium plate with the neutron convertor is placed at a distance of 1-5 mm from the mesh, defining the conversion (or drift) region of the detector. The chamber dimension is 15×25×5 cm$^3$, while for the slow detector with the polyethylene moderator it is 25×25×15 cm$^3$. The detectors can be deployed independently or as an assembly of one fast and one slow module (Figure 2). A total of 42 fast and 42 slow detectors will be deployed along the ESS accelerator mostly at the region of the MEBT, DTLs and Spokes [1, 2].

Each detector will be equipped with a front-end electronics card (FEE), which includes 2 FAMMAS current amplifiers (Fast Amplifier Module for Micromegas ApplicationS) [15], low voltage filters and two output driver buffers. The consumption of the card is less than 200 mW and allows the operation in both counting and current mode.

ISBN: 978-3-95450-202-8 doi:10.18429/JACoW-HB2018-THA1WE04



### *System Architecture*

The architecture of the ESS nBLM system is shown in Fig. 3. Besides the Micromegas detectors, it includes: the back-end electronics (BEE) and data acquisition system (DAQ), high and low voltage power supplies, the gas re-circulation system and the user interface and data archiving system. As with most other ESS diagnostic systems, the nBLM BEE is based on the MicroTCA.4 platform, while EPICS servers are used for the controls and monitoring.

The acquisition of the analogue signal of each detector is done by an IOxOS IFC_1410 AMC which is planned to be equipped with one IOxOS ADC_3111 FMC boards. Each FMC board has 8 channels and is acquiring data at 250 MS/s. The IFC carrier is equipped with FPGA devices which perform the real time signal processing without dead time. The Micromegas detector is a proportional avalanche chamber, where individual neutrons can create a pulse. The acquisition can be performed both in counting or current mode, passing automatically to each mode depending on the actual particle rate. A value of the number of counts and the current per µs, correlated to the beam loss can be used for the machine protection and monitoring purposes. The counting mode allows the monitoring of very low losses in long terms, while simulations performed with GEANT4 show that the detectors can give multiple counts within 1 µs when low energy protons are lost at level of 0.01 W/m.

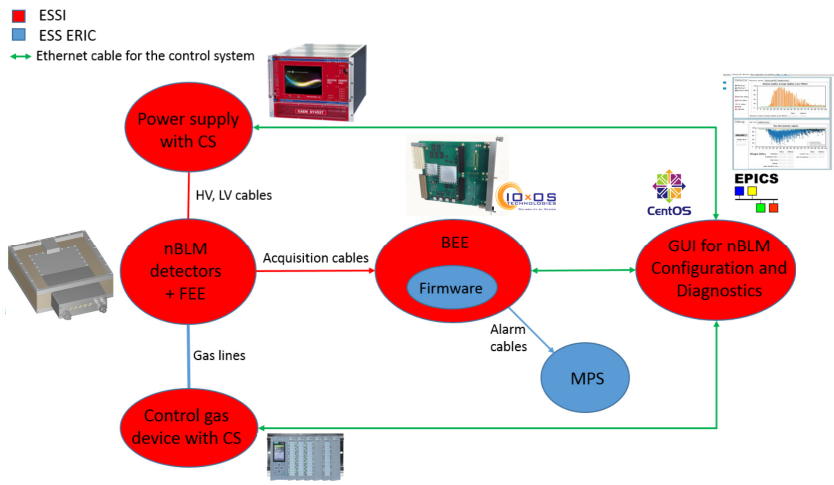


Figure 3: Architecture of the EPICS based Control System of ESS nBLM. The fast acquisition and the communication to ESS Machine Protection System is done by FPGAs running on a MicroTCA.4 platform.

In order to guarantee a stable operation on a time scale of years, the nBLM chambers will need a continuous flow of gas at the level of 0.1 l/h. The detectors will be grouped in series in six gas lines running along the linac. A PLC with Siemens S7-1500 CPU will be in charge of controlling and monitoring the gas flow. The detectors are designed to be able to perform stably for several hours in case the flow is interrupted, while the system will be able to detect a leak or the presence of impurities in the line and provide the health status to the EPICS GUI. The GUI will also control several CAEN SY4527 crates, which will be used to control the high and low voltage power supplies. The 48 channel CAEN A7030 cards will provide the HV on the mesh (-500V) and the drift (-700V) of each Micromegas detector in independent lines. The 8 channel CAEN A-2519 modules will be used to power the FEE cards, using 1 channel per group of 2-6 detectors.

## DETECTOR PERFORMANCE

The ESS nBLM is an innovative system that has not been used before in accelerator diagnostics. Thus, the response of the system to the ESS linac conditions can only be estimated based on Monte Carlo simulations and detector tests in other facilities.

The simulations that were performed during the design and optimization phase of the project have shown that, under different scenarios [2, 7], a full beam loss in the DTL region would imply a significant number of counts in the nearest detectors in the first µs after the loss (few tens when the loss is at the first DTL, $>10^4$ when at the last one) [16]. This response would allow the early signalization in case of accidental loss, while the relative response of the detectors deployed along the linac will provide information for the location of the loss. In the case of normal operation, the system will be sensitive to very low neutron fluxes, providing valuable data for material activation and beam tuning.

The actual calibration of beam losses as a function of the count rate will be done during the commissioning phase of the linac. Meanwhile, we have performed detector tests in several facilities in order to validate the simulations, optimize the design and provide a proof of principle. More tests are planned, including one in Linac4 by September 2018.

### *Efficiency for Neutrons - Gamma Suppression*

The AMANDE facility at IRSN [17], situated at Cadarache center, provides monoenergetic neutron fields, appropriate to measure the detection efficiency as a function of the neutron energy. The measurements (Figure 4) were performed in March 2018. The first results from the analysis allowed us to fix some parameters of the detectors, such

ISBN: 978-3-95450-202-8 doi:10.18429/JACoW-HB2018-THA1WE04

as the material of the neutron converter of the fast detector and the $B_4C$ layer thickness and the size of the polyethylene moderator of the slow one.

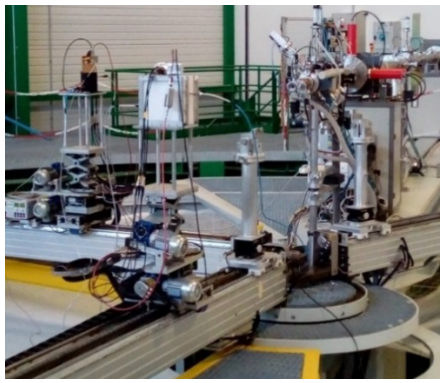

Figure 4: The setup at the AMANDE facility. The actual detector under testing is the slow one (white), while the fast one (black) was moved on the side.

The measured detection efficiency of the fast detector is shown in Fig. 5, and for the slow for different moderator thickness in Fig. 6. The efficiency of the slow detector is calculated taking into account the surface of the moderator ($25\times25$ cm$^2$) and not only the active area ($8\times8$ cm$^2$). This implies that the detector would give a count rate of few s$^{-1}$ for a neutron fluence rate of 1 s$^{-1}$cm$^{-2}$.

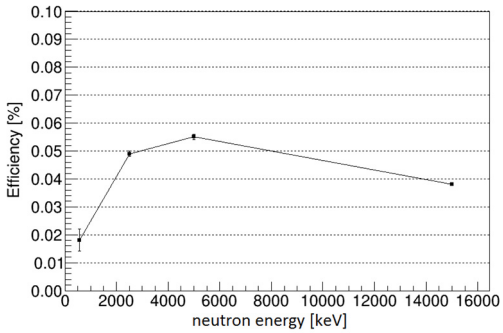


Figure 5: Neutron detection efficiency of the fast detector as a function of the neutron energy.

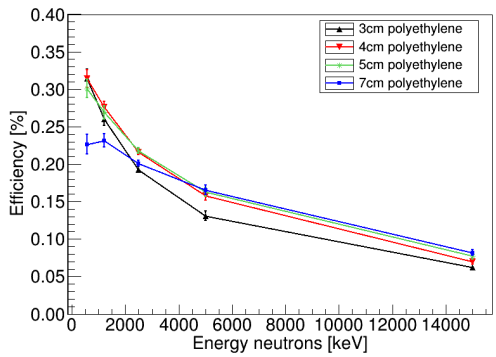


Figure 6: Neutron detection efficiency of the slow detector for different thicknesses of the polyethylene moderator.

In the case of 565 keV neutron field, a LiF target is used. There is therefore a contamination by 6-7 MeV gammas coming from the $^{19}F(p, \alpha\gamma)^{16}$ reaction. By using an $AlF_3$ target with the same thickness of fluorine, it is possible to isolate the response of the detector to gammas compared to the mixed field. The results are shown in Fig. 7 for the fast and in Fig. 8 for the slow detector.

Even though that 565 keV is very close to the lower limit of the sensitivity of the fast detector, it is clear that applying a threshold in the pulse amplitude it is possible to completely suppress the gammas while maintaining a good efficiency for the neutrons. As mentioned before, this suppression is an intrinsic characteristic of the detector and is due to the much higher ionization power of the proton recoils compared to the electrons that are produced by the gammas. It can be optimised with the choice of the operating voltages, the gas and the drift gap.

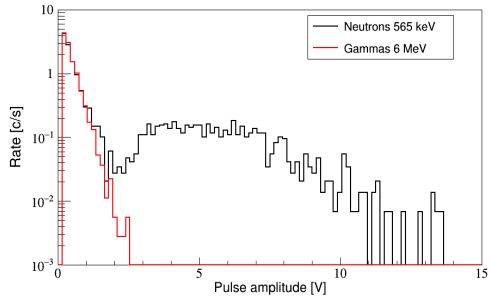


Figure 7: Response of the fast detector to the gammas from the $^{19}F(p, \alpha\gamma)^{16}O$ reaction and to the mixed field of gammas and 565 keV neutrons.

In the case of the slow detector the suppression is even stronger, because the ionization is caused by the α or $^7$Li particles emitted by the $^{10}B(n,\alpha)^7Li$ reaction. This allows us to reduce the drift gap (it was 0.4 mm compared to 2 mm for the fast) and the detector gain, suppressing thus the gammas even further. In parallel, since most of the reactions are caused by thermalized neutrons, the same suppression factor is possible independently of the initial energy of the incoming neutron.

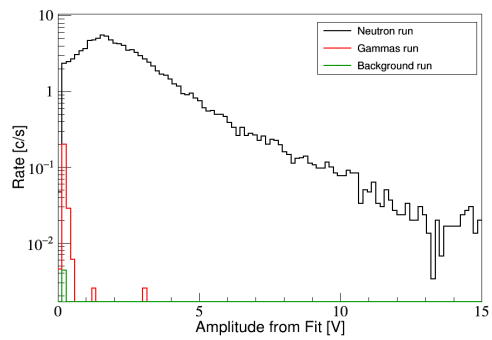


Figure 8: Response of the slow detector to the gammas from the $^{19}F(p, \alpha\gamma)^{16}O$ reaction and to the mixed field of gammas and 565 keV neutrons.

## *Time Response – Proof of Principle*

During the 1st quarter of 2018 a series of tests were performed at the IPHI proton beam at CEA Saclay [18]. In part of those tests, a Be target was used in order to produce a

ISBN: 978-3-95450-202-8 doi:10.18429/JACoW-HB2018-THA1WE04



neutron field. Both nBLM prototypes were used in order to measure the neutron flux distribution, but also to study the response of the detectors in a pulsed beam.

The energy of the proton beam was 3 MeV and the duration of a pulse about 90 µs, at a repetition frequency of 1 Hz. The data were taken using the FAMMAS amplifiers, which allowed us to study the pulse characteristics, (risetime, duration and amplitude distributions, noise) and develop the algorithms to be used in the FPGA of the ESS nBLM acquisition system.

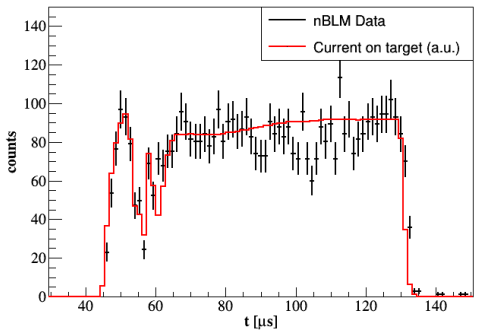


Figure 9: Time response of the fast detector in comparison with the intensity of current in the target.

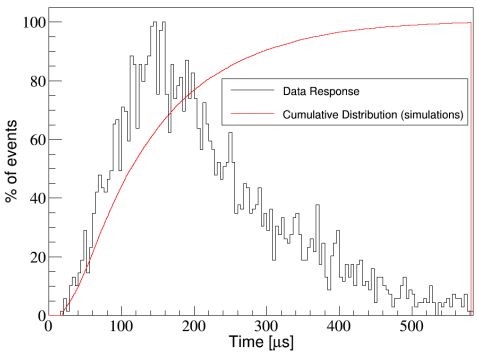


Figure 10: Time structure of the events in the slow detector following the 100 µs proton beam pulse. The response is slow due to the moderation time of the neutrons in the polyethylene, represented here by the red curve that shows the cumulative distribution of the events from a simulated instantaneous pulse.

The results verified the behavior predicted by the simulations [16]. The fast detector has an immediate response and the count rate is in direct correlation with the intensity of the beam current, as it was measured in the target (Fig. 9). In the case of the slow detector, due the moderation time most of the events are recorded with a delay of 100-200 ns. In Fig. 10 the simulated cumulative distribution of the recording time is represented in red, while the measured response to the IPHI pulse is shown in black. However, due to the much higher efficiency of the slow detector compared to fast, a significant number of the events (~5% of the total) will be register within the first µs, so also the slow detector can be used for an early warning in case of accidental beam loss.

We kept taking data with the nBLM prototypes at IPHI even when the Be target was replaced by an Al endcap, and the detectors were still able to register neutron counts. This is an important observation, showing that the detectors have the potential to see beam loses already at the region of the ESS MEBT ($E_p$ = 3.5 MeV).

A more systematic proof of principle came from the tests performed at the MC40 Cyclotron of Birmingham University [19], where we irradiated an Al plate with a 28 MeV proton beam. The correlation of the measured count rate and the beam intensity was linear and is shown in Fig. 11. Further tests are planned in order to quantify the neutron yield for materials that are used in the ESS linac.

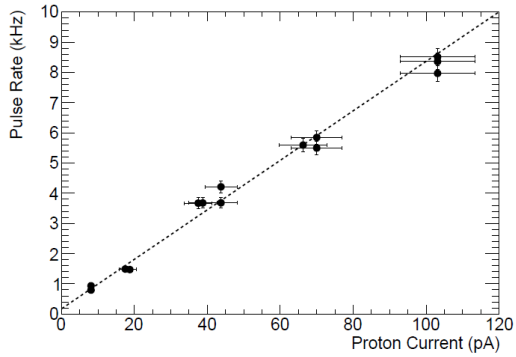


Figure 11: Correlation of the measured count rate with the intensity of the proton beam hitting an aluminium target.

The behaviour of the Micromegas under very high particle fluxes was studies in the facilities of the Orphée nuclear reactor at CEA Saclay. The slow detector, without the moderator, was exposed to 0.01 eV neutrons at a flux of $2\times10^6$ $s^{-1}$ $cm^{-2}$ operating stably, without discharges. The analysis of the results is ongoing, aiming to the optimization of the detector operation parameters.

## CONCLUSIONS

A new type of beam loss monitors is being developed for ESS, based on fast neutron detection with Micromegas detectors. The system is designed to operate both in event counting and current mode. Two types of detectors are used, one called “fast” and one “slow” in order to achieve fast reaction time to accidental beam losses, and enough sensitivity for long term activation protection and beam tuning. Both detectors have shown strong intrinsic gamma to neutron suppression capability.

## ACKNOWLEDGMENTS

The authors would like to thank Alain Menelle for his valuable help during the nBLM tests at the Orphée reactor the IRSN team at AMANDE facility.

L. Segui would like to acknowledge the financial support of Enhanced Eurotalents program (an FP7 Marie Skłodowska-Curie COFUND program).

R. Hall-Wilton, C. Höglund and L. Robinson would like to acknowledge financial support of the EU Horizon 2020 BrightnESS project, grant number 676548.

ISBN: 978-3-95450-202-8 doi:10.18429/JACoW-HB2018-THA1WE04

The project was supported by the French in-kind contribution to ESS and the H2020 project AIDA-2020, GA no. 654168.

## REFERENCES

[1] T. Shea *et al*., "Overview and Status of Diagnostics for the ESS Project", in *Proc. IBIC'17*, Grand Rapids, MI, USA, Aug. 2017, paper MO2AB2, doi:10.18429/JACoW-IBIC2017-MO2AB2

[2] I. Dolenc Kittelmann, "nBLM general overview", *ESS nBLM system CDR-1*, Lund, Sweden, Dec. 2017, https://indico.esss.lu.se/event/948/contribution/1/material/slides/0.pdf

[3] I. Dolenc Kittelmann, "Report on the MC simulations for the ESS BLM", ESS, Lund, Sweden, Rep. 0066428, Dec. 2016.

[4] V. Grishin, B. Dehning, A. Koshelev, A. Larionov, V. Seleznev and M. Sleptsov, "Ionization chambers as beam loss monitors for ESS linear accelerator," in *Proc. IBIC'17*, Grand Rapids, MI, USA, Aug. 2017, paper WEPWC03, p 54.

[5] A. Zhukov, Experience with the SNS loss monitoring and machine protection, in *Proc. PAC'13*, Pasadena, CA USA, paper WEYA2, p 714.

[6] J. Marroncle *et al*., "A New Beam Loss Monitor Concept Based on Fast Neutron Detection and Very Low Photon Sensitivity", in *Proc. IBIC'17*, Grand Rapids, MI, USA, Aug. 2017, doi: 10.18429/JACoW-IBIC2016-TUAL02

[7] I. Dolenc-Kittelmann and T. Shea, "Simulations and detector technologies for the beam loss monitoring system at the ESSlinac," in *Proc. HB'16*, Malmö, Sweden, July 2016, pp. 553–558.

[8] I. Giomataris, P. Rebourgeard, J.P. Robert, G. Charpak, "MICROMEGAS: a high-granularity position-sensitive gaseous detector for high particle-flux environments", *Nucl. Instrum. Meth. A*, vol. 376, p. 29, 1996.

[9] I. Giomataris, "Development and prospects of the new gaseous detector Micromegas", *Nucl. Instrum. Meth. A*, vol. 419 p. 239, 1998.

[10] F. Belloni, F. Gunsing, and T. Papapevangelou, "Micromegas for neutron detection and images", *Mod. Phys. Lett. A*, vol. 28, p. 1340023, 2013, https://doi.org/10.1142/S0217732313400233.

[11] C. Höglund, *et al*., "B4C thin films for neutron detection", *J. Appl. Phys.*, vol. 111, p. 104908, 2012.

[12] C. Höglund *et al*., "Stability of 10B4C thin films under neutron radiation", *Radiat. Phys. Chem*., vol. 113, p. 14, 2015.

[13] S. Schmidt, C. Höglund, J. Jensen, L. Hultman, J. Birch, and R. Hall-Wilton, "Low Temperature Growth of Boron Carbide Coatings by Direct Current Magnetron Sputtering and High Power Impulse Magnetron Sputtering", *Journal of Materials Science*, vol. 51, issue 23, 2016.

[14] I. Giomataris *et al*., "Micromegas in a bulk", *Nucl. Instrum. Meth. A*, vol. 560, pp. 405–408, 2006.

[15] P. Legou, "Beam Spectrometers using Micromegas in Time Projection Chamber mode", in *Proc. HB'06*, Tsukuba, Japan 2006, paper WEBZ03, p. 256.

[16] L. Segui, "Monte Carlo results: nBLM response to EES beam loss scenarios", Rep. CEA-ESS-DIA-RP-0023, July 2017.

[17] V. Gressier *et al*., "AMANDE: a new facility for monoenergetic neutron fields production between 2 keV and 20 MeV", *Rad. Prot. Dos.*, vol. 110, issue 1-4, Aug. 2004, https://doi.org/10.1093/rpd/nch185

[18] F. Senée *et al*, "Increase of IPHI beam power at CEA Saclay", presented at *IPAC'18*, Vancouver, Canada, Apr. 2018, paper TUPAF016, unpublished.

[19] P. Allport *et al*. Al., "Recent results and experience with the Birmingham MC40 irradiation facility", *JINST*, vol. 12, no. 03, p. C03075, 2017, doi: 10.1088/1748-0221/12/03/C03075